ECGI with a Deep Neural Network and 2D Normalized Body Surface Potential Maps

Tiantian Wang, Pietro Bonizzi, Joel Karel, Ralf Peeters

Department of Data Science and Knowledge Engineering, Maastricht University, Maastricht, The Netherlands

Abstract

Electrocardiographic Imaging (ECGI) reconstructs heart surface potentials (HSPs) from body surface potentials (BSPs) using a patient-specific torso-heart geometry derived from CT or MRI. Potential inaccuracies in the estimate of the torso-heart geometry, and of the electrode positions on the body surface may limit the accuracy of the reconstructed HSPs. In this study, we aim at providing a proof-of-principle Deep Neural Network (DNN) which directly maps BSPs to HSPs, without the need to estimate a transfer matrix for the forward problem. In particular, we propose a torso normalization method that can turn the original torso geometry into a 2D image, and transform it into a normalized body surface potential map (nBSPM). In this paper, we did this for four dog geometries. A 4-layer back propagation (BP) neural network is built and trained with the nBSPMs as the input, and the pixel values of corresponding heart surface potential maps (HSPMs) as the output. The experiments show that the mean-squared error (MSE) on the validation data set decreases and converges to around 3.0. The value of the Pearson correlation coefficient between the original and reconstructed HSPMs on the test data set is larger than 0.92. This indicates that the proposed model is suitable for reconstructing HSPs from BSPs.

1. Introduction

In recent years, different deep learning methods have been developed to solve the inverse problem in electrocardiographic imaging (ECGI). As a noninvasive technique, reconstructing heart surface potentials (HSPs) from body surface potentials (BSPs) with a deep neural network (DNN) has a large potential to be applied in cardiac diagnosis. However, in several studies [1] [2], the deep learning techniques were designed without accounting for different geometries of both torso and heart. When using directly the original BSP and HSP values as the input/ouptut in DNN, extra effort is needed to deal with the network structure and to find suitable parameters.

In this paper, we propose a torso normalization method to generate 2D normalized body surface potential maps (nBSPMs). This is used as input to a neural network, so that the network can be sufficiently independent of a specific patient's geometry. With heart surface potential maps (HSPMs) expanded from BullsEye plots [3] as the output, we also build a 4-layer deep neural network.

2. Torso normalization method

In this preliminary work, the torso normalization process is developed for a dog geometry. Firstly, an 'opening electrode' is selected on the torso back by observing the spatial relationship between torso and heart. Secondly, through cylinder coordinate transformation and setting the value of the radius to 1, the original torso geometry is turned into a unit cylinder. Thirdly, from an opening line, the cylinder surface is unfolded into a 2D image on which the BSPs on each time instant are plotted. Missing values of electrodes were interpolated with the average potentials of the neighboring electrodes.

2.1. Opening electrode

First of all, a coordinate system is chosen with its origin at the center of gravity of the torso geometry, and its Z-axis parallel to the spinal cord (Figure 1). The body surface electrode closest to the intersection point between the coordinate axis in the direction chest-back and the torso back is selected as the opening electrode.

2.2. Conversion of the torso geometry to a unit cylinder

To unfold the torso geometry into a 2D image, all the electrodes should be mapped to the same plane. Firstly, after locating the opening electrode, the coordinates of all electrodes (x, y, z) are turned into $(\varphi, r, z) = (atan2(y, x), \sqrt{x^2 + y^2}, z)$ by transforming the Cartesian coordinates to cylinder coordinates. Then by setting the

radius to $r = 1$, a unit cylinder (Figure 2) with coordinates $(atan2(y, x), 1, z)$ is achieved. As a result, all electrodes are placed on the cylinder surface. Secondly, we rotate the whole cylinder around the Z-axis so that the angle of the opening electrode becomes $\varphi = 0$. A line going through the opening electrode and parallel to the Z-axis is set to be the opening line.

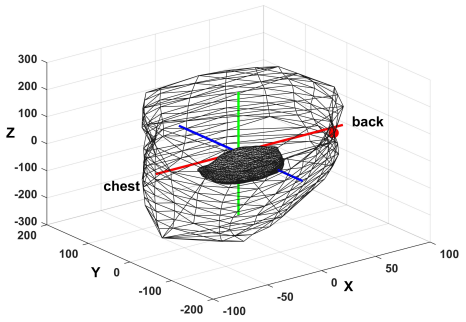

Figure 1. Selection of the opening electrode (red point). The center of gravity of the torso is the origin of the coordinate system. X axis corresponds to chest-back direction.

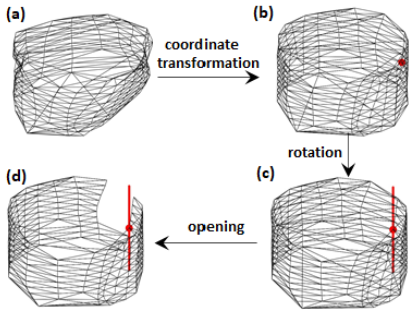

Figure 2. Process of opening the torso geometry. Original torso (a) is converted to a unit cylinder (b) through coordinate transformation and by setting the radius to 1. Then the angle of the opening electrode is turned into 0 through rotation (c). The cylinder is opened along the opening line (d). Red line is the opening line.

2.3. Unfolding and interpolation

After conversion to a unit cylinder and rotation of the opening electrode, the torso geometry can be unfolded into a 2D image, and the coordinate values (x', y') of the 2D image are achieved by letting $x' = atan2(y, x)$, $y' = z$. Therefore, the values on the new X-axis range from 0 to 2π with the values of the opening line equal to 0. The opening line turns out to be the side of the 2D image, thus the chest is shown in the middle area of the image. Missing values are then interpolated by averaging the values at neighboring electrodes. Figure 3 shows the interpolated results on four different time instants of two different dogs.

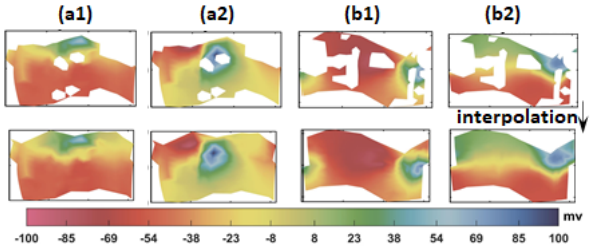

Figure 3. Interpolation results. (a1) (a2) are BSPs on two time instants from one torso geometry. (b1) (b2) are from a different torso geometry. On the first row are the original BSPs, on the second row the interpolated BSPs. The potential map is placed in a minimal enclosing rectangle with the boundary filled with white. Each map has a width of 2π and a length of torso height.

3. Experiments

3.1. Data preparation

In this study we used the same data set as in [4]. Briefly, in 4 normal anesthetized dogs, 2 silicone bands with 99 electrodes were implanted around the basal and mid-basal ventricular epicardium. Additional electrodes were placed at the LV apical epicardium, the LV endocardium, the RV apical endocardium, and the right atrial endocardium, providing a total of 103 electrodes. After chest closure, body-surface electrodes (184 to 216, depending on torso size) were attached to the chest. In the four dogs, 92 different beats were recorded, including 6 sinus beats and 86 paced beats.

Before generating potentials maps, BSPs and HSPs of each beat were normalized to [-100, 100](mv) in order to share the same colorbar. Then following the torso normalization process, the 2D nBSPM was generated for each time instant of each individual beat. To generate corresponding 2D HSPMs, we start from the data at the mesh points underlying the BullsEye plots proposed in [3]. The polar coordinates were transformed back into Cartesian coordinates to obtain rectangular plots as in nBSPM, see Figure 4. In order to be used in DNN, we converted the nBSPMs and HSPMs from RGB images to gray images, and resized it to 30x40 and 20x30, then finally converted it to 1200x1 and 600x1 vectors respectively. As a result, an nBSPM vector together with an HSPM vector on each time instant is set as an input/output pair of pixel values, for a total of 16361 different image pairs (different time instants) used in this study.

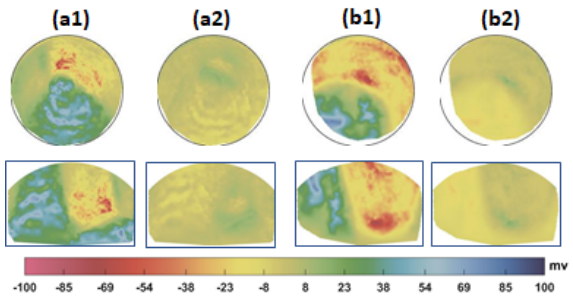

Figure 4. From Bullseye plot to HSPMs. (a1) (a2) are HSPs on two time instants from one heart geometry. (b1) (b2) are from a different heart geometry. On the first row are the Bullseye plots, on the second row the corresponding HSPMs. Each HSPM is placed in an minimum enclosing rectangle with the boundary filled with white. To show it more clearly, the HSPM is stretched since the original one has a width of 2π and a length of 1. (different time instants from Figure 3)

3.2. Back Propagation neural network

Reconstructing HSPMs directly from nBSPMs can be seen as a regression problem with multi-dimensional input and output. Although the convolutional neural network is often the first choice when it comes to image data, the size of convolution kernel, the number of convolution layers, the type of optimizer as well as some training parameters all need to be determined, which lead to unnecessary complexity while designing the network structure. In this study, we chose to use the back propagation (BP) neural network and reshaped the image matrix into a vector. Theoretically, we can approximate any function with a single hidden layer by increasing the number of nodes [5], but better results were achieved when adding one more hidden layer. Based on our experiments, a 4-layer BP neural network with 1200 nodes in the input layer, 800 nodes in the first hidden layer, 50 nodes in the second hidden layer and 600 nodes in the output layer was used. The sigmoid function is chosen as the activation function after the two hidden layers and output layer.

Among 16361 pairs of nBSPMs/HSPMs, 15261 pairs from 86 different beats, 709 pairs from 4 different beats and 391 pairs from 2 different beats were used for training, validation and test respectively. The meaning of introducing validation data is to select 'candidate networks' which are then evaluated on test data, thus an optimal network model can be determined. It should be mentioned that the value range of both nBSPMs and HSPMs are $[0, 1]$, therefore there is no need to normalize the data before inputting it to the neural network. While training, 500000 iterations with the number of randomly sampled nBSPMs/HSPMs equal to 200 on each iteration were implemented, and the validation was done every 250 iterations. In addition, the initial weights on each layer were sampled from the standard uniform distribution on the interval (-0.5, 0.5). The learning rate was set to be 0.1. Because of the ill-posedness of the regression problem, Tikhonov regularization was included in the mean-squared error (MSE) loss function with the regularization parameter equal to 0.00002.

4. Results

Figure 5 shows how the MSE varies on validation data during the iteration process. The loss decreases from around 6.5 to 2.1. 10 different network models with MSE lower than 2.1 are selected to measure the performance on test data. Among the 10 models, the one with lowest MSE on test data is used as the final network.

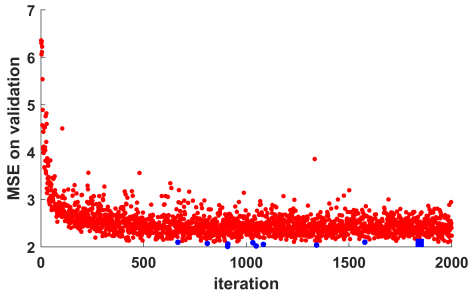

Figure 5. Mean-Squared Error (MSE) of validation data. It decreases from around 6.5 to 2.1. 10 scatter points are shown in blue (both dot and square) with MSE lower than 2.1. One scatter point is shown in square with lowest MSE on test data.

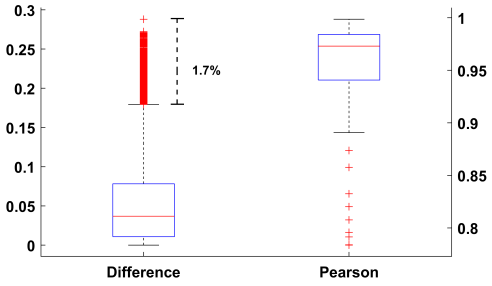

Figure 6. Boxplot of the test results. The left boxplot shows the difference between each output node and ground truth node for all 391 test samples, and the percentage of outliers is denoted. The right boxplot shows the Pearson correlation coefficient between original and reconstructed HSPMs for all 391 test samples.

Applying the final network to the test data set, the MSE value is 1.82, and Figure 6 shows the boxplots of test results. The boxplot of the difference between each output

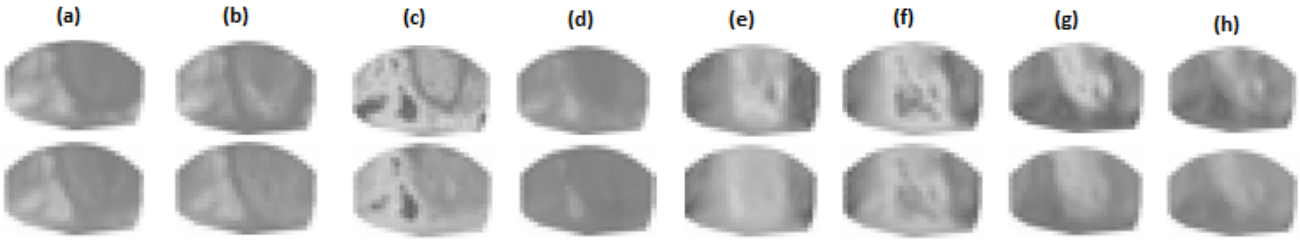

Figure 7. Original and reconstructed HSPMs. (a) (b) (c) (d) (e) (f) (g) (h) are eight time instants on two beats different from beats used in training and validation. The first row are the original HSPMs, the second row are reconstructed HSPMs.

node and ground truth node for all 391 test samples is depicted on the left, for a total of 234600 scatter points are included. The median is 0.04. Those values bigger than 0.18 are set to be the outliers, made up of only 1.7% of the total nodes number. The right boxplot shows the Pearson correlation coefficient between original and reconstructed HSPMs for all 391 test samples, ranging from 0.89 to 1 with 9 outliers bigger than 0.78. Figure 7 depicts the original and reconstructed HSPMs on 8 different time instants. Each output achieves a shape similar to the original HSPM, yet with a bit blurry border. Although some detailed information is lost in the output, the general potential distribution is relatively similar to the original HSPMs.

5. Discussion and conclusion

In this paper, we propose a torso normalization method which can turn the 3D BSPs to 2D potential maps, and developed a back propagation neural network that reconstructs HSPMs using nBSPMs for dog data, with the pixel values of each map being the input and output. As a step for generating the data set used by the neural network, the proposed torso normalization method unifies the way for accessing the standardized potential maps for different torso geometries, making sure the chest part is in the middle area of the map. The original Bullseye plots of heart geometry is expanded to HSPMs based on coordinate transformation, which can maintain the geometry differences as nBSPMs. The proposed normalization allows to avoid accounting for patient specific torso and heart geometries, and the corresponding differences among those, thus making it easier for the neural network to capture a generic relation between torso and heart potentials. For the test results, the value of Pearson correlation coefficient between original and reconstructed HSPMs is greater than 0.89, which suggests that the trained network can predict HSPMs well for new nBSPMs.

For future work, we plan to apply this methodology to human data. The impact of different torso geometries, and the behaviour of different types of beats will be further explored.

Acknowledgments

I would like to thank Job Stoks for helping with the implementation of the Matlab code to generate BullsEye plots in batches.

Tiantian Wang is funded by the China Scholarship Council (CSC), grant number 201908210340.

References

[1] Malik A, Peng T, Trew ML. A machine learning approach to reconstruction of heart surface potentials from body surface potentials. In 2018 40th Annual International Conference of the IEEE Engineering in Medicine and Biology Society (EMBC). IEEE, 2018; 4828–4831.

[2] Karoui A, Bendahmane M, Zemzemi N. Direct mapping from body surface potentials to cardiac activation maps using neural networks. In 2019 Computing in Cardiology (CinC). IEEE, 2019; Page–1.

[3] Stoks J, Chau Nguyen U, Peeters R, Volders P, Cluitmans M. An open-source algorithm for standardized bullseye visualization of high-resolution cardiac ventricular data: Unisys. Computing in Cardiology December 2020;47:1–4. ISSN 2325-8861.

[4] Cluitmans MJ, Bonizzi P, Karel JM, Das M, Kietselaer BL, de Jong MM, Prinzen FW, Peeters RL, Westra RL, Volders PG. In vivo validation of electrocardiographic imaging. JACC Clinical Electrophysiology 2017;3(3):232–242.

[5] Hornik K, Stinchcombe M, White H. Multilayer feedforward networks are universal approximators. Neural networks 1989;2(5):359–366.

Address for correspondence:

Tiantian Wang
Department of Data Science and Knowledge Engineering, Maastricht University, P.O. Box 616, 6200 MD, Maastricht
tiantian.wang@maastrichtuniversity.nl